Journal of Materials Chemistry C

PAPER

Cite this: J. Mater. Chem. C, 2018, 6, 1255

Carbon nanotube-assisted synthesis of ferromagnetic Heusler nanoparticles of Fe_3Ga (Nano-Galfenol)†

Rasha Ghunaim, *[ab] Victoria Eckert,[a] Maik Scholz, [a] Markus Gellesch,[ac] Sabine Wurmehl,[ad] Christine Damm, [a] Bernd Büchner,[ad] Michael Mertig [be] and Silke Hampel[a]

Received 10th October 2017, Accepted 8th January 2018

DOI: 10.1039/c7tc04618a

rsc.li/materials-c

A new type of Heusler nanoparticles of the formula Fe_3Ga has been prepared by facile synthesis approaches using pre-fabricated multi-walled carbon nanotubes. The tubes act as a template and a coating to protect the magnetic material from oxidation and agglomeration. For the purpose of comparison, the Fe_3Ga bulk material was also prepared by a novel method from the metal precursors. The morphology, structural determinations and the magnetic properties of both types of materials are presented. Compared to the bulk material, an enhancement in coercivity was observed for the nanoparticles which make them excellent candidates for magnetic storage devices. Since bulk Galfenol is a known magnetostrictive material, it is worth studying the effect of downsizing this material to the nanoscale dimension on such properties.

1. Introduction

Heusler compounds, a particular type of intermetallic alloys, which are ternary compounds that have the general formula of X_2YZ, where X and Y are transition metals and Z is a main group element.[1] These compounds were named after Fritz Heusler who discovered ferromagnetic behavior in Cu_2MnAl, although none of the individual elements from which the material is composed of are ferromagnets.[2]

Heusler compounds constitute a large family of highly functional and versatile intermetallic materials. While many of these compounds are studied in the form of single- or polycrystalline bulk samples or thin films, not much is known about their properties and functionalities when prepared in the form of nanoparticles. However, for numerous potential applications, *e.g.* in spintronics, the nanoscale dimension of the material cannot be neglected.[3]

Galfenol, an alloy of iron substituted with non-magnetic gallium, offers desirable properties such as tensile strength and magnetostrictive strains on the order of 100 MPa and 100×10^{-6}, respectively, which make them promising candidates for a mechanically strong actuator and sensing materials used for the design of shock-prone environmental transducers.[4,5]

However, the chemical, physical, magnetic, or optical properties of a given material are size-dependent;[6,7] thus, it is worth studying the effect of downsizing to the nanoscale dimension on, *e.g.* the magnetic properties. Due to the finite size of the nanoparticles and the high surface-to-volume ratio, these particles are highly subjected to oxidation and agglomeration.[8,9] In addition, size control is a challenge, particularly when particles are prepared by harsh methods such as ball milling.[10,11] Basit *et al.* applied a wet chemistry method, in which Heusler nanoparticles (of the type Co_2FeGa) were precipitated on a porous silica matrix where a poor size distribution was also observed.[12] A very interesting study has been carried out for the Co_2FeGa Heusler system,[13] where the material has been synthesized in a wet chemical way by the use of carbon nanotubes (CNTs) as templates. For the Fe_3Ga Heusler system (Galfenol), many investigations exist for the bulk material, but to the best of our knowledge, none for Fe_3Ga nanoparticles.

In this work, we successfully synthesized Fe_3Ga magnetic nanoparticles (MNPs). Based on the studies of Gellesch *et al.*, we used carbon nanotubes (CNTs) as templates, in which the MNPs are encapsulated inside the inner hollow cavity of the CNTs. These tubes provide a shell to protect MNPs from

[a] Leibniz Institute for Solid State and Material Research Dresden, Helmholtzstrasse. 20, 01069 Dresden, Germany. E-mail: r.ghunaim@ifw-dresden.de; Tel: +49 (0) 351 4659 413
[b] Institute for Physical Chemistry, Technische Universität Dresden, 01062 Dresden, Germany
[c] School of Physics and Astronomy, University of Birmingham, Birmingham B15 2TT, UK
[d] Institute for Solid State Physics, Technische Universität Dresden, 01062 Dresden, Germany
[e] Kurt-Schwabe-Institut für Mess- und Sensortechnik e. V. Meinsberg, 04736, Waldheim, Germany

† Electronic supplementary information (ESI) available. See DOI: 10.1039/c7tc04618a

oxidation, prevent agglomeration, and are a beneficial tool to control the size of the encapsulated MNPs, since the upper limit of the encapsulated MNP diameter will be the diameter of the inner cavity of the CNTs.

For the purpose of comparison, the bulk material was also prepared. To this aim, nitrate salts as metal precursors were mixed with the respective stoichiometry and reduced to the corresponding metals similar to the nanomaterials. The magnetic properties for the prepared Fe_3Ga nanoparticles and the bulk were compared with data published by Kawamiya *et al.* in 1972.[14]

2. Experimental part

2.1. Preparation of nanoparticles inside CNTs

Multi-walled carbon nanotubes (MWCNTs) of the type PR-24-XT-HHT (Pyrograf Products, Inc., Cedarville OH, USA) have been used as templates or 'nano-containers' for the preparation of intermetallic nanoparticles. This type of CNTs is distinguished by their high purity which results from the fact that the as-produced carbon nanotubes are heat treated to 3000 °C which reduces the iron content (*i.e.* the growth catalyst) to a very low level (<100 ppm).[15–17] The Fe_3Ga@CNTs have been prepared by the following two filling approaches.

The first approach is an extension of a reported solution filling approach for CNTs[18] in which 1 M standard aqueous solutions of the following nitrates were prepared: $Fe(NO_3)_3{\cdot}9H_2O$ (grade: ACS 99.0–100.2%) and $Ga(NO_3)_3{\cdot}xH_2O$ (grade: ACS 99.99% metal basis) supplied by VWR Chemicals and Alfa Aesar GmbH & Co KG (Karlsruhe, Germany). The nitrate salts were used as provided and the water content of the gallium nitrate salt was calculated to be $x \approx 7$ *via* thermogravimetric analysis (TGA). This result is in a good agreement with literature reports.[19,20] The solutions were combined in a stoichiometric ratio with respect to the metal ions (*i.e.* Fe : Ga = 3 : 1), and about 50 mg of MWCNTs were added and the mixture was treated in an ultrasonication bath for 1 h at room temperature. The mixture was then vacuum-filtered and washed with about 20 ml of the washing agent of acetone and distilled water at a volumetric ratio of 1 : 1. The solid residue was then dried for 24 h at a temperature of 108 °C and reduced under hydrogen and argon atmospheres (50 vol% Ar + 50 vol% H_2) at a temperature of 500 °C for 4 h to convert all the nitrates and oxides into the corresponding metallic state. An additional heat treatment step was essential to obtain the desired intermetallic phase, in which the reduced samples were further annealed under a mixture of H_2 and Ar gas streams (95 vol% Ar + 5 vol% H_2) at a temperature of 680 °C for 48 h. This might be a very important step in order to ensure particle growth and obtain a homogeneous composition and a well-ordered crystalline structure of intermetallic MNPs.[21]

In an attempt to obtain a relatively higher degree of filling, the second approach was followed, in which the nitrate precursors were directly mixed with the specific amount of CNTs in a sealed round-bottom flask. A few drops of distilled water were added to ensure good stirring. The flask with the mixture was placed in an oil bath and heated to a temperature of around $T \approx 80$ °C for 4 h. The mixture was then naturally cooled down to room temperature and washed with about 20–30 ml of the washing agent of acetone and distilled water at a volumetric ratio of 1 : 1. The samples were then dried, reduced and annealed in a manner similar to the solution filled samples. This approach differs from that of the solution one, in the way that the liquid medium of the filling material is provided with a higher saturation (due to the absence of water solvent), which increases the percentage of the material that fills the CNTs.

2.2. Preparation of the Fe_3Ga bulk material

For the synthesis of the bulk material, we slightly modified the second approach, in which the iron and gallium nitrates were mixed at a 3 : 1 stoichiometry in a sealed round-bottom flask placed in an oil bath and heated for 4 h at 80 °C. The mixture was then dried for 24 h at 108 °C and reduced at a temperature of 680 °C for 4 h under H_2 and Ar atmospheres (50 vol% Ar + 50 vol% H_2). Thereafter, the sample was annealed at the same temperature for 40 h under a mixture of H_2 and Ar gas streams (95 vol% Ar + 5 vol% H_2).

2.3. Characterization

All samples were routinely investigated by scanning electron microscopy (SEM) with a Nova 200 NanoSEM (FEI) operated at 15 kV and combined with an energy-dispersive X-ray (EDX) analyzer (AMETEK). The SEM samples were prepared by placing a thin film of the sample on a carbon tape. Transmission electron microscopy (TEM), high-resolution transmission electron microscopy (HRTEM) measurements and nanobeam electron diffraction were performed using a Tecnai F30 (FEI) operated at 300 kV or a Tecnai G2 (FEI) operated at 200 kV. Both are equipped with an EDX analyzer (AMETEK, Oxford). The TEM samples were prepared by adding a few drops of the sample suspension in acetone on a copper grid with a carbon coating on one side.

Crystal structure identification for the bulk material and magnetic nanoparticles inside CNTs was done using a STADI P (STOE) X-ray diffractometer (XRD) with Mo Kα radiation (λ = 0.70930 Å) in transmission geometry at a scanning rate of 0.01° s^{-1} in the 2θ range from 10° to 80°. An extra crystal structure identification measurement for the nanoscale sample was performed using an X′Pert Pro MPD PW3040/60 X-ray diffractometer (XRD) (PANalytical) with Co Kα radiation (λ = 1.79278 Å) in reflection geometry at a scanning rate of 0.05° s^{-1} in the 2θ range from 10° to 80°.

Thermogravimetric measurements (TGA) were performed using a SDT-Q600 (TA Instruments). A few milligrams of the material (~5 mg) were heated to a temperature of 900 °C at a heating rate of 5 K min^{-1} followed isothermally for 15 minutes under an air atmosphere at a flow rate of 100 ml min^{-1}.

The magnetic field dependence of magnetization at 5 K and 300 K in an external magnetic field of up to ±5 T was measured by using a superconducting quantum interference device (MPMS-XL SQUID) magnetometer from Quantum Design (San Diego, CA, USA). The samples were filled inside gelatin

capsules, and the diamagnetic contribution of the sample holder and the empty CNTs was subtracted.

3. Results and discussion

3.1. Morphology and structure

The morphology and geometry of the filling material and its location inside CNTs were examined by SEM (Fig. 1).

Fig. 1a shows an overview image in back-scattered electron (BSE) mode for the as-prepared sample from the first (*i.e.* solution) filling approach. The filling particles are distributed along the inner cavity of the hollow CNTs. For samples prepared by the second filling approach (Fig. 1b), the same behavior is observed, however with a seemingly higher degree of filling compared to the solution approach. This can be seen from the pearl necklace-like appearance of the filling inside the CNTs and was confirmed by quantitative measurements performed by TGA as will be shown later.

It is important to emphasize on the effect of annealing on the growth of the particles. For the as-prepared samples (*i.e.* only reduced) (Fig. 1a and b), different morphologies and particle sizes for the filling materials have been observed (small spheres, large spheres, and agglomerates as indicated by arrows in Fig. 1b), whereas after an additional heat treatment step (annealing for about 48 h) a significant growth in the particles' size has been observed. This observation was confirmed by the statistical measurements of the particles' aspect ratio and their diameter with respect to the diameter of the inner walls of the CNTs. Fig. 1c and d show SEM overview images in BSE mode and SE mode, respectively, for a sample prepared by the second filling approach after an additional heat treatment step. We attribute the observation of a pronounced increase in particle size for a prolonged heat treatment (*i.e.*, annealing for 48 h) to the availability of a significantly higher amount of thermal energy, which increase the probability of particle merging, which in turn leads to particle growth.

TEM measurements were performed for samples prepared by both filling approaches, for each of the as-prepared and annealed samples. Fig. 2a shows an example of an as-prepared sample of Fe_3Ga@CNTs prepared by the second filling approach, in which most of the particles are located within the hollow cavity of the CNTs and exhibit a wide variety of sizes. All particles have diameters much lower than the inner diameter of the CNTs, whereas after further heat treatments (Fig. 2b) most of the particles reached a diameter nearly equal to that of the inner walls of the CNTs.

The morphology of the individual nanoparticles for the annealed sample was highlighted by HRTEM measurement (Fig. 2c). The crystallinity of the core material was confirmed by the appearance of the lattice fringes (the region marked as a red square), in which the fcc structure of Fe_3Ga can be identified from an interplanar distance of 0.207 nm (220).

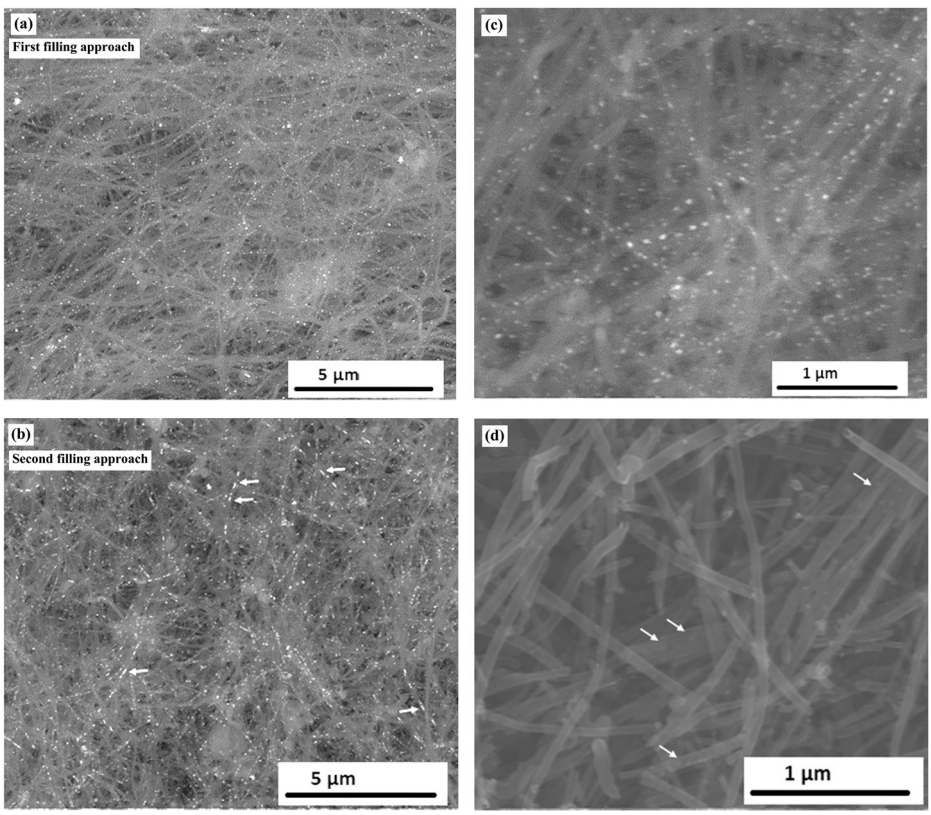

Fig. 1 SEM overview image in BSE mode in contrast to the as-prepared sample prepared by (a) first (solution) filling and (b) second filling approaches. The samples after annealing in (c) BSE mode and (d) topography (SE) mode, where the particles can also be seen as indicated by arrows (second filling approach).

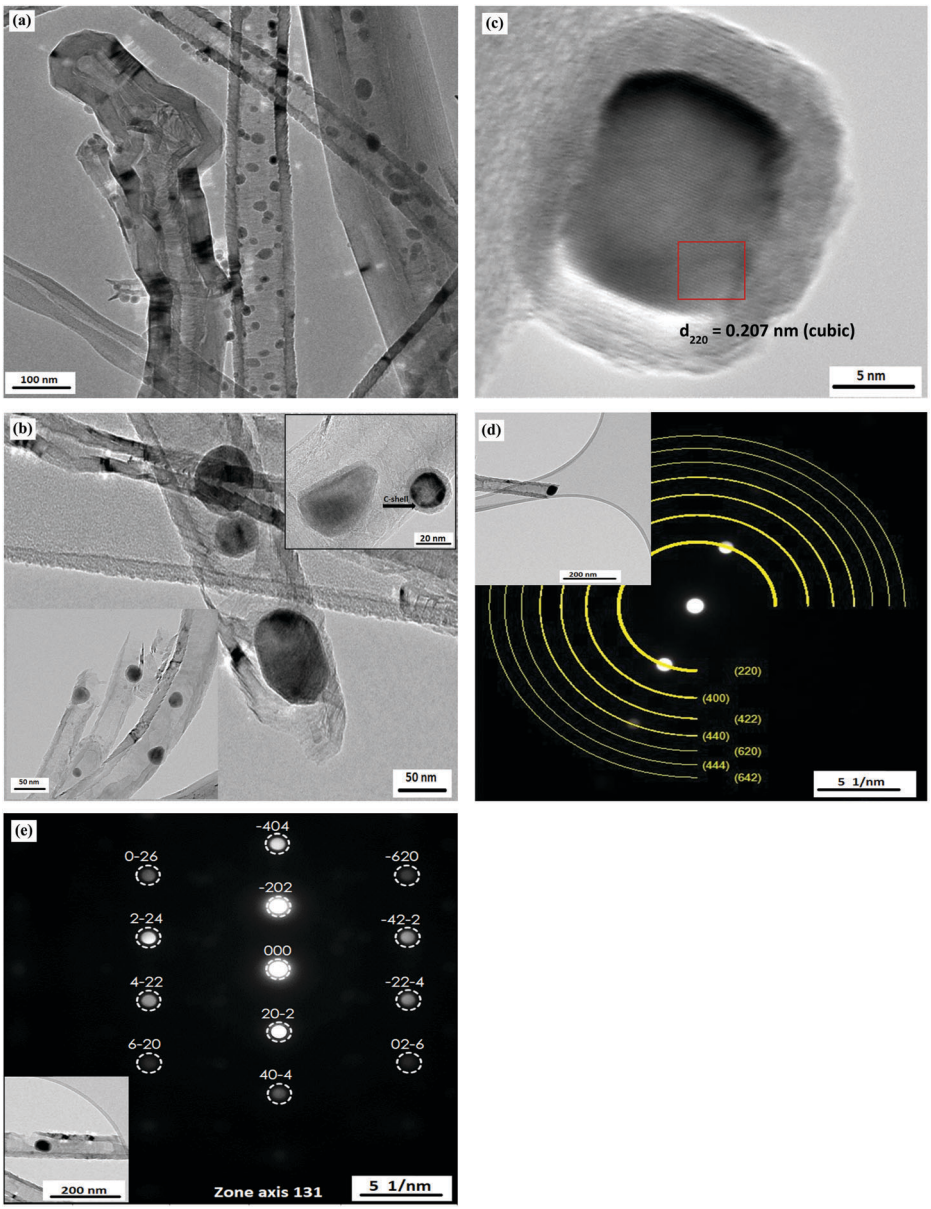

Fig. 2 TEM bright-field images of CNTs filled with Fe_3Ga nanoparticles (second filling approach): (a) as-prepared and (b) after annealing for 48 h (upper-right corner: MNP attached to the outer surface of the CNTs and covered with a C-shell that originates from carbon coating during TEM observations). (c) HRTEM image of Fe_3Ga nanoparticles with the corresponding lattice fringes. (d) Ring diagram and (e) electron diffraction patterns of Fe_3Ga nanoparticles with the corresponding TEM images as insets. The diffractogram was obtained for the zone axis [131].

For the as-prepared samples, no such well-defined crystalline structure could be clearly observed in HRTEM images. We attribute this observation to the inhomogeneity of the sample, lack of crystallinity, and the presence of different phases inside CNTs. This finding underlines that a further annealing step is essential to obtain well-defined intermetallic nanoparticles.

TEM-based nanobeam electron diffraction was carried out for several individual nanoparticles of the annealed sample (Fig. 2d and e insets), revealing that the filling particles are single crystalline with a Heusler-type $L2_1$ lattice structure, as indicated by the reflections corresponding to the 220 (0.205 nm), 440 (0.102 nm) and 422 (0.117 nm) (Fig. 2d and e) lattice planes which coincide with the bulk material. This is a clear confirmation of the formation of the Heusler-type Fe_3Ga phase.

The distribution of the particles' diameter was investigated for the as-prepared and annealed filled samples prepared by the second approach. The diameters were measured perpendicular to the long axis of the CNTs. The as-prepared samples have a mean diameter of $d_{NP} = d_{TEM} = 18 \pm 6$ nm (Fig. 3a), whereas the annealed samples having a mean diameter of $d_{NP} = d_{TEM} = 40 \pm 10$ nm was calculated (Fig. 3b). These values were compared with the mean diameter of the hollow cavity of the

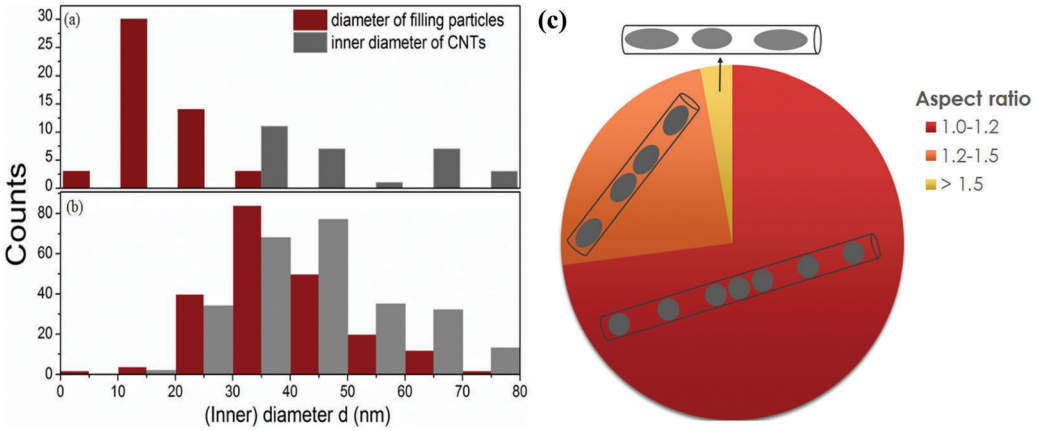

Fig. 3 Histograms representing the distribution of the inner diameters (nm) of CNTs and particle diameters for the (a) as-prepared and (b) annealed samples. (c) Schematic representation of the geometry of the filling particles of the annealed sample with respect to the aspect-ratio values (a colored version of this figure can be viewed online).

CNTs (d_{CNT} = 47 ± 15 nm). The confinement principle was applicable, in which the CNT inner cavities limit the particle size and to a large extent prevent particle agglomeration in both samples. Furthermore, a strong divergence between the size distribution of the as-prepared and annealed samples is obvious. Hence, for very regular particles with high homogeneity and crystallinity, an annealing step is necessary.

The spherical geometry of the intermetallic nanoparticles inside CNTs was confirmed by aspect-ratio calculations (*i.e.* the ratio of the particle's long axis to its short axis). 73% of the filling particles in a sample having nearly 250 investigated filling particles had a ratio of about 1.0–1.2, whereas only 24% of the particles had an aspect ratio in the range of 1.2–1.5, and only the remaining 3% exhibited a ratio larger than 1.5. The largest observed ratio was 1.7. Fig. 3c shows a schematic representation of the geometry of the filling particles based on the aspect ratio values.

The expected stoichiometry of 3 : 1 for the binary Heusler compound was confirmed by EDX measurement, in which the EDX analyzer was attached to both SEM and TEM. In SEM-EDX, the stoichiometry was obtained by measuring the relative ratio of the individual elements over an analyzed area of about 60 × 50 μm^2 (see Fig. S1 in the ESI†), whereas in TEM-EDX, the relative ratio was obtained for a large number of individual nanoparticles. Quantitative analysis indicates atomic percentages of Fe (73.07 ± 1.40 at%) and Ga (26.93 ± 1.40 at%) in the Fe_3Ga@CNT samples.

XRD measurements were performed for all samples prepared by both filling approaches, whereas only for the annealed samples we could clearly identify the phase-pure Heusler compound Fe_3Ga. The XRD pattern for the annealed Fe_3Ga@CNT prepared by the second approach is shown in Fig. 4a, where the intense reflection at $2\theta \sim 12^\circ$ corresponds to the 002 lattice plane of the CNTs (labeled C). The reflections at $2\theta \sim 20^\circ$, 28°, 35° and 41° correspond to the lattice planes 220, 400, 422 and 440, respectively, of the Fe_3Ga Heusler structure with space group $Fm\bar{3}m$ (225, cubic, PDF No. 04-003-6567 (Mo-anode material)). No reflections corresponding to oxides or carbides were detected.

For the purpose of comparison, the bulk material of Fe_3Ga has been prepared by a novel method from the metal precursors. The XRD diffraction pattern for the bulk sample was measured and compared to that of the nanoparticles (Fig. 4a). Rietveld refinement identifying the exact structure of the material was also carried out as displayed in Fig. 4c.

An additional XRD measurement was also performed for the annealed Fe_3Ga@CNT sample using a X′Pert X-ray diffractometer (Co Kα = 1.79278 Å). The XRD pattern is shown in Fig. 4b, where the intense reflections at $2\theta \sim 30^\circ$ and 37° correspond to the CNT lattice planes 002 and 102, respectively (labeled C). The reflections at $2\theta \sim 51^\circ$ and 76° correspond to the lattice planes 220 and 400, respectively, of the Fe_3Ga Heusler structure with space group $Fm\bar{3}m$ (225, cubic, PDF No. 04-002-1175 (Co-anode material)).

Assuming the spherical shape of these nanoparticles and using Scherrer's equation, $D = 0.93\lambda/\Delta(2\theta)\cos(\theta)$, where D is the mean size of the particles, λ is the X-ray wavelength and $\Delta(2\theta)$ is the line broadening at half the maximum intensity (FWHM) in radians,[22] the mean particle diameter d_{XRD} equals to 29.3 ± 0.2 nm, which correlates well with the mean particle size obtained from the statistical analysis of the TEM measurements (d_{TEM} = 40 ± 10 nm) and confirms the high crystallinity of the material (Fig. 3b).

A comparison between the lattice parameters of the bulk sample and the reference material was also calculated and listed in Table 1 (data obtained from the Inorganic Crystal Structure Database (ICSD)).[23]

TGA is mainly used as an indication of the sample purity (*i.e.* the absence of outside particles which exhibit an increase in mass prior to the combustion of the CNTs) and for the determination of the magnetic content of the material inside the CNTs based on the mass residue calculations. This measurement confirms the observations found by SEM that the main difference between the two filling approaches is the filling yield, *i.e.*, samples prepared by the second filling approach are found to have a higher filling yield in comparison with those prepared by the first (solution) filling approach. For some samples, the filling yield

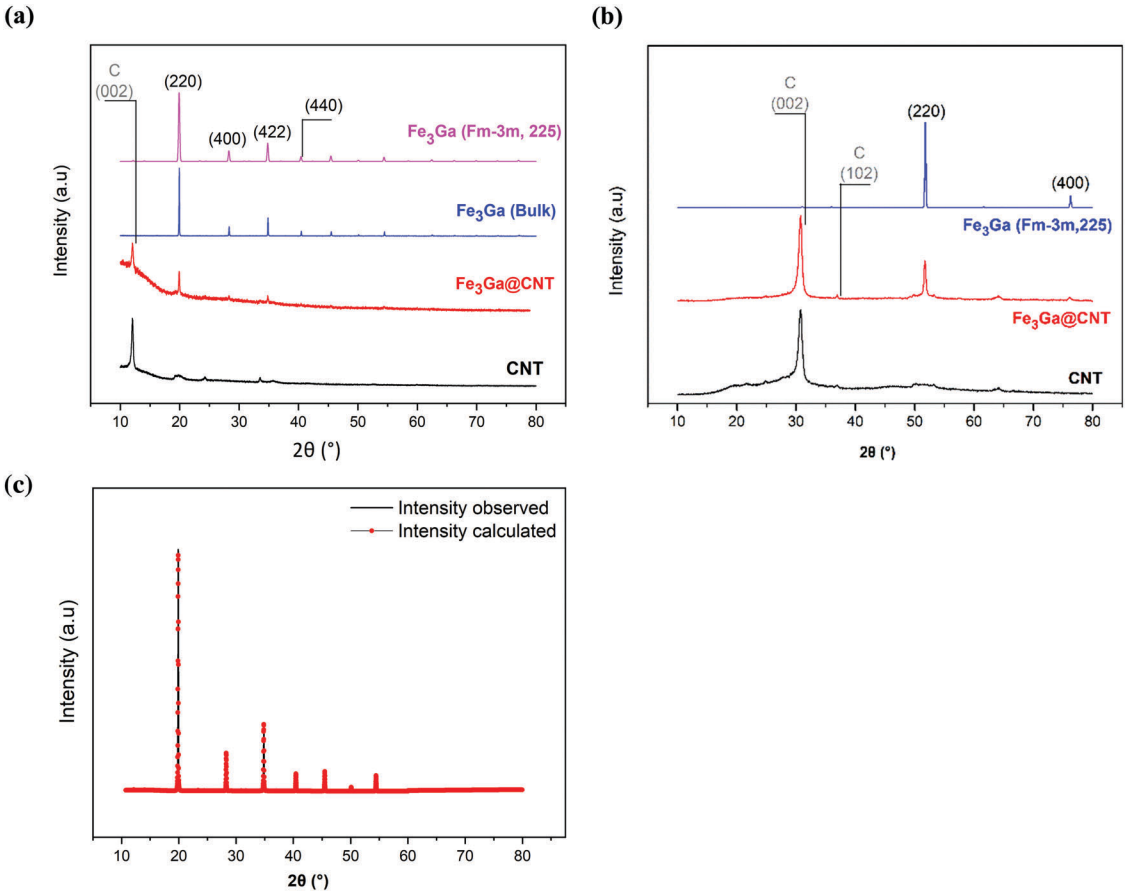

Fig. 4 XRD diffraction patterns for the annealed sample of Fe_3Ga@CNT (second filling approach) in comparison with the standard Fe_3Ga, (a) Mo-anode material (PDF No. 04-003-6567), (b) Co-anode material (PDF No. 04-002-1175) and (c) Rietveld refinement for the bulk material (a colored version of this figure can be viewed online).

Table 1 Comparison between the lattice parameters of the prepared bulk sample and the reference material of Fe_3Ga with space group $Fm\bar{3}m$, 225. (PDF No. 04-003-6567)

Lattice parameters	Bulk sample (observed)	Fe_3Ga ($Fm\bar{3}m$, 225)
a	5.80145 Å	5.807 Å
b	5.80145 Å	5.807 Å
c	5.80145 Å	5.807 Å
α, β, γ	90.000°	90.000°

reached ~8.7 wt% for solution-filled samples (Fig. 5, black curve), whereas for the samples prepared by the second approach, the filling yield was as high as 11.2 wt% (Fig. 5, purple curve). The lower filling yield of the solution-filled samples can be attributed to the occupancy of the inner volume of the CNTs by water, which decreases the filling capacity of the inner CNT cavity, compared to the available filling volume in the second filling approach, in which only a few drops of distilled water is required, solely to ensure good stirring. The humped peak observed for the samples filled by the second approach indicates the presence of some particles attached to the outer surface of the CNTs, nevertheless, they are coated with carbon layers (see the inset in Fig. 2b, upper-right corner). Therefore, no diffraction peaks for the corresponding oxides were observed as shown by XRD measurements.

3.2. Magnetic properties

As mentioned in the Introduction, one of the main points of this work was to study the effect of reduction of the Fe_3Ga alloy to the nanoscale size on their magnetic properties in comparison to the bulk material. The magnetic properties of the encapsulated MNPs and the produced bulk material were compared with those results obtained by Kawamiya *et al.* for a sample prepared from pure iron and gallium elements sealed into an evacuated quartz tube and heated to a temperature over 1000 °C for about 3 days.[14]

The magnetic field dependence of the magnetization $M(H)$ has been measured for the bulk material, as-prepared and annealed samples prepared by the second filling approach at 5 K (Fig. 6a). The saturation magnetization M_s for the bulk material was about 165.7 emu g^{-1}, a value correlating well with that obtained by Kawamiya *et al.* at 4.2 K (~169.0 emu g^{-1} for the fcc phase), whereas for the annealed Fe_3Ga@CNT nanoparticles, M_s equals to 152.2 emu g^{-1}. This finding implies that the relative high saturation magnetization known for the bulk material is preserved even for the Fe_3Ga Heusler nanoparticles. Furthermore, the magnetization data give evidence for the importance of the annealing step since the as-prepared sample exhibits a M_s significantly lower than the reported data for the

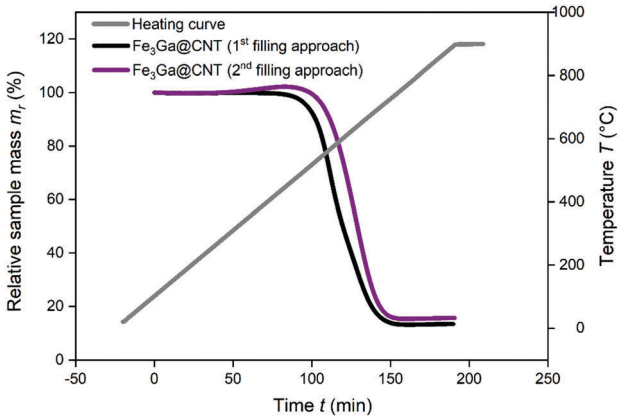

Fig. 5 Relative sample mass loss for the sample filled by the first approach (*i.e.* solution) (black) and the other filled by the second approach (purple) of Fe_3Ga@CNTs during the combustion process of the nanocomposite, in which mass of the CNTs starts to decrease at $T \sim 530$ °C (a colored version of this figure can be viewed online).

bulk material (117.0 emu g^{-1}). This can be attributed to a lower crystallinity of the MNPs for the as-prepared samples compared to the annealed samples and the bulk material, and the formation of a bulk-like ferromagnetic core and a shell composed of disordered moments[9,24] (therefore, HRTEM for the as-prepared MNPs was not possible, as has been shown earlier).

The temperature dependencies of the saturation magnetization for the bulk material and the annealed sample indicated a change of less than 4% when going from 5 K to 300 K. This weak decrease in the saturation magnetization with an increase in temperature from 5 K to 300 K can be attributed to the generally high Curie temperature (T_c) of bulk Heusler compounds and particularly of Fe_3Ga.[13] In other words, both the saturation magnetization and T_c of the bulk material are preserved in the Fe_3Ga Heusler nanoparticles. The field-dependent magnetization data measured at 300 K are shown in Fig. S2 in the ESI.†

The measured saturation magnetization enables the assessment of the content of the ferromagnetic material in Fe_3Ga@CNTs. The value of the saturation magnetization is governed by the magnetic properties of the MNPs which we estimate by the bulk value and the amount of the ferromagnetic material with respect to the diamagnetic CNTs (*i.e.* $M_s^{MNP@CNT}/M_s^{bulk}$). This comparison indicates a filling yield of approximately 10.1 wt%, which correlates well with the TGA results ($\sim$11.2 wt%). In other words, the mass fraction of the magnetic active material is about 10–11 wt% for Fe_3Ga@CNTs.

Unlike saturation magnetization, coercivity is a size-dependent property already in the size range studied here. The data in Fig. 6 demonstrate a robust enhancement in the hardness of the magnetic nanoparticles compared to the bulk material. The coercive field (H_c) measurement for the annealed samples of Fe_3Ga nanoparticles prepared by the second filling approach at 5 K gave $H_c \approx 433$ Oe. This value is approximately nine times higher than the bulk material at the same temperature (H_c-bulk $\sim$ 50 Oe) (Fig. 6b).

The increase in the coercive field as the particle size decreases can be attributed to the size dependence of coercivity in the vicinity of the critical size of domain formation in nanoparticles.[25–27] In short, the regime coercivity of single-domain (SD) magnets decreases upon size reduction while it increases in the multi-domain (MD) state. The fact that the as-prepared samples have significantly larger coercivities compared to the annealed ones can hence be straightforwardly attributed to the small size of the MNPs stabilizing the SD state. The fact that larger post-annealed MNPs exhibit smaller coercive fields can hence be associated with the MD state realized in such large particles.

4. Conclusions

In this work, a new type of Heusler nanoalloys of the formula Fe_3Ga has been prepared using carbon nanotubes as templates for the formation of nanoparticles. Our study demonstrates that

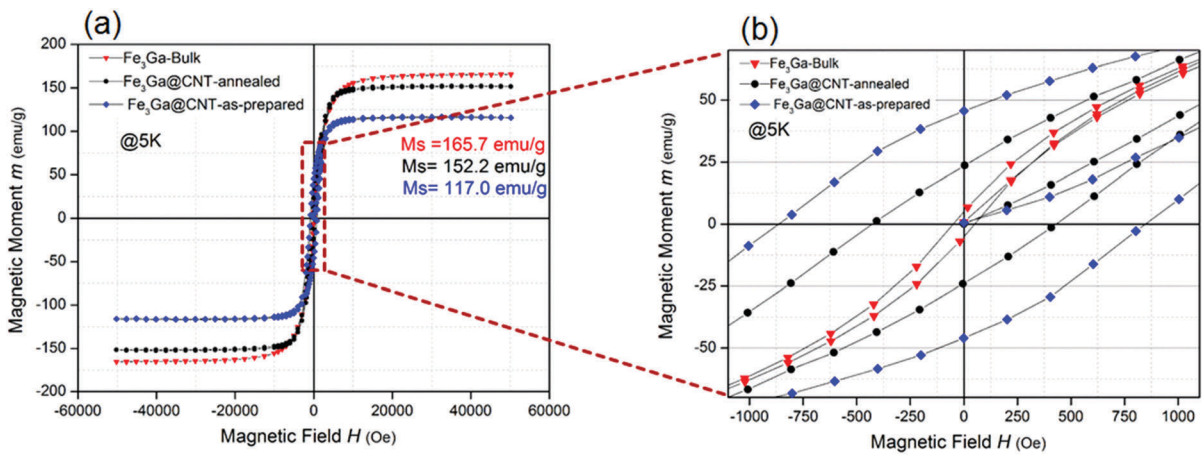

Fig. 6 (a) Hysteresis curves, measured at 5 K, for the Fe_3Ga bulk material in comparison to the Fe_3Ga@CNT nanoparticles. (b) Enlarged view of the hysteresis curves shows the enhancement of the coercive field for the Heusler nanoparticles compared to the bulk material (a colored version of this figure can be viewed online).

both wet chemistry techniques offer a facile way to synthesize Heusler nanoparticles in a well-defined manner. The additional annealing process is mandatory for phase pure, high crystalline Fe_3Ga@CNTs. In addition, we were able to prepare the bulk material by a novel method from the salt precursors. The magnetic properties of the magnetic nanoparticles were measured. It was found that saturation magnetization is preserved even at the nanoscale, whereas the hardness of the Fe_3Ga@CNTs was enhanced due to size reduction. This approach of filling and preparing of nanoalloys opens the door for many materials to be re-sized down to the nanoscale dimensions for the discovery of unique new properties, which can be significantly different from their bulk counterpart, and hence, new applications can emerge.

Conflicts of interest

There are no conflicts to declare.

Acknowledgements

The authors thank C. Nowka and R. Heider for support with XRD measurements and Rietveld refinement, G. Kreutzer for TEM measurements and S. Gaß for support with magnetic measurements. RG acknowledges the German Academic Exchange Service (DAAD), MG acknowledges support from the Studienstiftung des deutschen Volkes and SW acknowledges the Deutsche Forschungsgemeinschaft (project WU595/3-3) for funding.

References

1 T. Graf, C. Felser and S. S. P. Parkin, Simple rules for the understanding of Heusler compounds, *Prog. Solid State Chem.*, 2011, **39**, 1–50.
2 F. Heusler, *Verhandlung der Deutschen physikalischen Gesellschaft*, Friedr. Vieweg & Sohn, 1903, vol. 5, p. 219.
3 C. Felser, G. H. Fecher and B. Balke, Spintronics: A challenge for Materials Science and Solid-State Chemistry, *Angew. Chem., Int. Ed.*, 2007, **46**, 668–699.
4 R. A. Kellogg, *Development and modeling of iron-gallium alloys*, Iowa State University, Ames, Iowa, 2003.
5 A. E. Clark, J. B. Restorff, M. Wun-Fogle, T. A. Lograsso and D. L. Schlagel, Magnetostrictive properties of body-centered cubic Fe–Ga and Fe–Ga–Al alloys, *IEEE Trans. Magn.*, 2000, **36**, 3238–3240.
6 G. Guisbiers, Size-dependent materials properties toward a universal equation, *Nanoscale Res. Lett.*, 2010, **5**, 1132–1136.
7 E. Roduner, Size matters: why nanomaterials are different, *Chem. Soc. Rev.*, 2006, **35**, 583–592.
8 C. Bantz, O. Koshkina, T. Lang, H.-J. Galla, C. J. Kirkpatrick, R. H. Stauber and M. Maskos, The surface properties of nanoparticles determine the agglomeration state and the size of the particles under physiological conditions, *Beilstein J. Nanotechnol.*, 2014, **5**, 1774–1786.
9 B. Issa, I. M. Obaidat, B. A. Albiss and Y. Haik, Magnetic nanoparticles: surface effects and properties related to biomedicine applications, *Int. J. Mol. Sci.*, 2013, **14**, 21266–21305.
10 Y. D. Wang, Y. Ren, Z. H. Nie, D. M. Liu, L. Zuo, H. Choo, H. Li, P. K. Liaw, J. Q. Yan, R. J. McQueeney, J. W. Richardson and A. Huq, Structural transition of ferromagnetic Ni_2MnGa nanoparticles, *J. Appl. Phys.*, 2007, **101**, 063530.
11 K. Vallal Peruman, M. Mahendran, S. Seenithurai, R. Chokkalingam, R. K. Singh and V. Chandrasekaran, Internal stress dependent structural transition in ferromagnetic Ni-Mn-Ga nanoparticles prepared by ball milling, *J. Phys. Chem. Solids*, 2010, **71**, 1540–1544.
12 L. Basit, C. Wang, C. A. Jenkins, B. Balke, V. Ksenofontov, G. H. Fecher, C. Felser, E. Mugnaioli, U. Kolb, S. A. Nepijko, G. Schönhense and M. Klimenkov, Heusler compounds as ternary intermetallic nanoparticles: Co_2FeGa, *J. Phys. D: Appl. Phys.*, 2009, **42**, 084018.
13 M. Gellesch, M. Dimitrakopoulou, M. Scholz, C. G. F. Blum, M. Schulze, J. van den Brink, S. Hampel, S. Wurmehl and B. Büchner, Facile nanotube-assisted synthesis of ternary intermetallic nanocrystals of the ferromagnetic Heusler phase Co_2FeGa, *Cryst. Growth Des.*, 2013, **13**, 2707–2710.
14 N. Kawamiya, K. Adachi and Y. Nakamura, Magnetic properties and Mössbauer investigations of Fe-Ga alloys, *J. Phys. Soc. Jpn.*, 1972, **33**, 1318–1327.
15 PR-24-XT-HHT Data Sheet retrieved from http://pyrograf products.com/nanofiber.html#_PR-24-XT-HHT_Data_Sheet, accessed October 2017.
16 M. Arlt, D. Haase, S. Hampel, S. Oswald, A. Bachmatiuk, R. Klingeler, R. Schulze, M. Ritschel, A. Leonhardt, S. Fuessel, B. Büchner, K. Kraemer and M. P. Wirth, Delivery of carboplatin by carbon-based nanocontainers mediates increased cancer cell death, *Nanotechnology*, 2010, **21**, 335101.
17 J.-P. Tessonnier, D. Rosenthal, T. W. Hansen, C. Hess, M. E. Schuster, R. Blume, F. Girgsdies, N. Pfänder, O. Timpe, D. Sheng Su and R. Schlögl, Analysis of the structure and chemical properties of some commercial carbon nanostructures, *Carbon*, 2009, **47**, 1779–1798.
18 S. C. Tsang, Y. K. Chen, P. J. F. Harris and M. L. H. Green, A simple method of opening and filling carbon nanotubes, *Nature*, 1994, **372**, 159–162.
19 W.-S. Jung, Preparation of gallium nitride powders and nanowires from a Gallium(III) nitrate salt in flowing Ammonia, *Bull. Korean Chem. Soc.*, 2004, **25**, 51–54.
20 V. Berbenni, C. Milanese, G. Bruni and A. Marini, Thermal decomposition of gallium nitrate hydrate $Ga(NO_3)_3.xH_2O$, *J. Therm. Anal. Calorim.*, 2005, **82**, 401–407.
21 M. Gellesch, *Statistical study of the effect of annealing treatments on assemblies of intermetallic magnetic nanoparticles related to the Heusler compound Co_2FeGa,* Technische Universität Dresden, IFW-Dresden, Germany, 2015.
22 A. L. Patterson, The Scherrer formula for X-ray particle size determination, *Phys. Rev.*, 1939, **56**, 978–982.
23 https://www.fiz-karlsruhe.de/de/leistungen/kristallographie/icsd.html, accessed October 2017.
24 E. M. M. Ibrahim, L. H. Abdel-Rahman, A. M. Abu-Dief, A. Elshafaie, S. K. Hamdan and A. M. Ahmad, Electric,

thermoelectric and magnetic characterization of γ-Fe_2O_3 and Co_3O_4 nanoparticles synthesized by facile thermal decomposition of metal-Schiff base complexes, *Mater. Res. Bull.*, 2018, **99**, 103–108.

25 A. Akbarzadeh, M. Samiei and S. Davaran, Magnetic nanoparticles: preparation, physical properties, and applications in biomedicine, *Nanoscale Res. Lett.*, 2012, **7**, 144.

26 J. S. Lee, J. M. Cha, H. Y. Yoon, J.-K. Lee and Y. K. Kim, Magnetic multi-granule nanoclusters: A model system that exhibits universal size effect of magnetic coercivity, *Sci. Rep.*, 2015, **5**, 12135.

27 E. F. Kneller and F. E. Luborsky, Particle size dependence of Coercivity and Remanence of single–domain particles, *J. Appl. Phys.*, 1963, **34**, 656–658.